

# The Active Galaxy 3C 66A: A Variable Source of Very High-Energy Gamma-Rays

Yu. I. Neshpor, A. A. Stepanyan, O. R. Kalekin, N. A. Zhogolev, V. P. Fomin,  
N. N. Chalenko, and V. G. Shitov

*Crimean Astrophysical Observatory, p/o Nauchnyi, Crimea, 334413 Ukraine*

Received September 20, 1999

**Abstract**—Observations of the very-high-energy gamma-ray flux of the blazar 3C 66A ( $z = 0.444$ ) carried out at the Crimean Astrophysical Observatory with the GT-48 atmospheric Cerenkov detector are reported. The gamma-ray fluxes in 1997 and 1998 were lower than in 1996. The optical luminosity of the object in 1997–1998 also decreased in comparison with its value in 1996. If the emission is isotropic, the very-high-energy gamma-ray power is  $10^{46}$  erg/s. © 2000 MAIK “Nauka/Interperiodica”.

## 1. INTRODUCTION

Blazars—active galactic nuclei whose prototype is BL Lac—are probable extragalactic sources of gamma rays with very high energies (VHE,  $E > 10^{11}$  eV). These objects are very interesting astrophysically, because they are characterized by substantial flux variations at all wavelengths from radio to X-rays. In some cases, large-amplitude X-ray variations coincide with optical variations [1]. The timescales of the variations are from minutes to about one year. Blazars are distinguished by a strong tendency for flaring (with timescales of several days) and outburst activity (with durations of several months). This suggests that these objects contain a large number of high-energy particles, which can generate VHE gamma rays when they interact with matter or electromagnetic fields.

The first such objects from which VHE gamma rays were detected were the BL Lac objects Mrk 421 and Mrk 501 [2, 3]. The related active galaxy 3C 66A was detected optically [4] as a 15th magnitude pointlike blue source. Its optical emission is strongly polarized, with the degree of polarization varying widely with time, sometimes reaching 30%. The brightness of the object also varies appreciably with time; for instance, it exceeded  $14^m$  in 1996.

High-energy gamma rays were detected toward 3C 66A at energies  $> 100$  MeV by EGRET, and the gamma-ray source was given the name 2EG J0220+4228. The position error of the EGRET measurement was  $1^\circ$  [6]. Additional measurements of the gamma-ray flux from this direction allowed the source position to be determined to higher accuracy. In the third EGRET catalog [7], this object was listed as the gamma-ray source 3EG J0222+4253 with coordinates  $\alpha = 35^\circ 7'$  and  $\delta = 42^\circ 9'$ , which differ from the coordinates of 3C 66A by  $0^\circ 15'$ .

We detected VHE gamma rays from the blazar 3C 66A in 1996 in our observations on the GT-48 Cerenkov

detector [8]. The observations were continued in 1997 and 1998. The results of the three-year flux measurements are presented below.

## 2. BRIEF DESCRIPTION OF THE GT-48 GAMMA-RAY TELESCOPE

Gamma rays with energies  $E > 10^{11}$  eV can be detected using ground-based equipment, using the fact that VHE gamma rays interact with the nuclei of atoms in the air, generating so-called electron–photon showers. These are made up of high-energy electrons and positrons, which emit optical Cerenkov radiation, primarily at small angles ( $0.5^\circ$ – $1^\circ$ ) to the direction of motion of the primary photon. This makes it possible to determine the direction from which the flux of gamma rays arrives.

The effective area in which Cerenkov events from electron–photon showers can be detected is rather large. The region on the Earth covered by an event with vertical incidence of the primary particle is approximately  $4 \times 10^8$  cm<sup>2</sup>; i.e., it forms a circle with a diameter of 250 m. This makes it possible to detect small (approximately  $10^{-11}$  photons cm<sup>-2</sup> s<sup>-1</sup>) gamma-ray fluxes.

The main obstacle to detecting and studying VHE gamma-ray sources is the presence of an appreciable cosmic-ray background, whose particles cause Cerenkov events in the Earth’s atmosphere that are difficult to distinguish from those due to discrete gamma-ray sources. Nevertheless, there are some differences between these two types of events. Currently, multielement receiving cameras are used to make images of Cerenkov events. Differences in the parameters of the images of Cerenkov events resulting from gamma rays and from cosmic-ray particles enable us to eliminate most of the latter events.

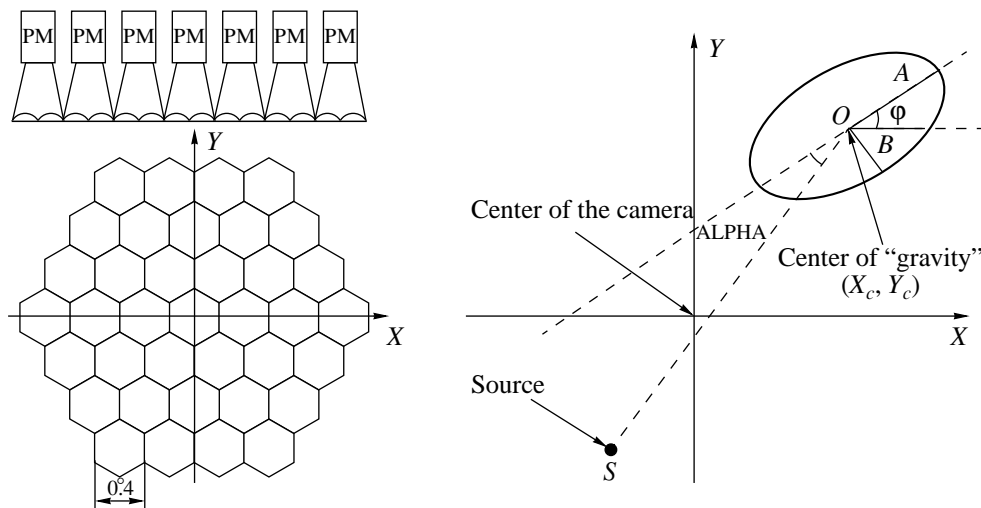


**Fig. 1.** Schematic representation of the light detector and parameters of a Cerenkov event.  $A$  is the effective length and  $B$  the effective width of the event image,  $\varphi$  is the orientation angle,  $\text{ALPHA}$  is the azimuthal angle, and PM is the photomultiplier.

The first telescope with a multichannel camera began operation at the Whipple Observatory (USA) in 1982 [9]. A similar telescope, GT-48, started working at the Crimean Astrophysical Observatory in 1989. We have described the GT-48 telescope in a number of papers (see, for example, [10]). The facility consists of two identical northern (1) and southern (2) altitude–azimuth mounts (sections) separated by 20 m in the north–south direction at a height of 600 m above sea level. We showed in [11] that, in contrast to single telescopes, a double telescope operating in a coincidence regime can almost completely eliminate events due to individual charged particles hitting the light detectors.

Six aligned telescopes are mounted on each section. The optics of each telescope consist of four 1.2-meter mirrors with a common focal point. The mirrors of three telescopes have a focal length of 5 m. Light detectors (cameras) consisting of 37 photomultipliers (37 cells) that can image Cerenkov events at visual wavelengths (300–600 nm) are located in their focal plane. Events are recorded only when the amplitudes of time-coincident signals in any two of the 37 cells exceed a preset threshold. The time resolution of the coincidence circuit is 15 ns.

There is a conical hexagon-shaped light-guide in front of each photomultiplier. The mean diameter of the entrance window corresponds to the linear angle of the field of view of one cell,  $0.4^\circ$  (Fig. 1). The field of view of the entire light detector is  $2.6^\circ$ .

The other three telescopes have focal lengths of 3.2 m and are intended for detection of the ultraviolet radiation of Cerenkov events at 200–300 nm. The detectors are sun-blind photomultipliers.

The total area of the mirrors on both mountings (sections) is  $54 \text{ m}^2$ . The installation can be moved by a control system with a drive accuracy of  $\pm 1'$ . Observa-

tions can be carried out both in a coincidence regime using the two sections and independently by each section. The effective threshold energy for detection of gamma rays is 1.0 TeV.

### 3. OBSERVATIONS AND DATA PROCESSING

Observations of 3C 66A ( $\alpha = 2^\circ 22' 40''$ ,  $\delta = 43^\circ 02' 08''$ ) were carried out in 1996, 1997, and 1998 using the two sections in a coincidence regime with a time resolution of 100 ns. We tracked the object and an area of sky (background) at the same azimuth and zenith angles with a 30-min time shift between trackings (the duration of a single observation was 25 min). The observations of the background preceded those of the source.

In total, we processed the data for 12 sessions in 1996, 30 in 1997, and 17 in 1998, corresponding to a total duration for the observations of 3C 66A of 1175 min (24 h 35 min). We performed a preliminary reduction of the data, necessary for correct calculation of the first and second moments of the brightness distribution, from which we derived the parameters of the Cerenkov events: effective length  $A$ , effective width  $B$ , angle  $\varphi$  describing the direction of maximum elongation of the image (i.e., its orientation), and the coordinates  $X_c$  and  $Y_c$  of the center of “gravity” of the brightness distributions (Fig. 1). We calculated the moments for cells whose signal exceeded a certain threshold value [12]. All other parameters of a Cerenkov event can be derived from these parameters [10].

As a result of our preliminary reduction, there remained over the three years of observations 34 695 source events and 34 770 background events for further analysis. Thus, the difference of the number of source ( $N_s$ ) and background ( $N_b$ ) events  $N_\gamma = N_s - N_b = -75 \pm 264$ , where 264 is the statistical error. This includes a contri-

bution from transparency variations. To determine the probable gamma-ray flux, we must eliminate events due to the charged cosmic-ray component.

We noted above that the parameters of Cerenkov events due to VHE gamma rays differ little from those due to charged cosmic-ray particles. Nevertheless, by excluding events due primarily to cosmic rays, we can considerably reduce the error in the difference in the number of source and background events. This requires correct choice of the boundary values of the selection parameters, in order to optimize the signal-to-noise ratio  $Q = (N_{0_s} - N_{0_b}) / \sqrt{N_{0_s} + N_{0_b}}$ , where  $N_{0_s}$  and  $N_{0_b}$  are the numbers of gamma-like events in the on-source and background observations. The difference  $N_{0_s} - N_{0_b} = N_\gamma$  is the selected number of gamma rays detected during the observations, and  $\sqrt{N_{0_s} + N_{0_b}}$  is the statistical error of the signal determination after selection. If the selection is done using several parameters, it is possible to exclude up to 99% or more of events due to the charged cosmic-ray component.

When analyzing the 1996 data in [8], we used the parameter DRO, which characterizes the magnitude of the stereoscopic effect. Selecting according to this parameter, we could detect the flux of VHE gamma rays from 3C 66A at the  $5.1\sigma$  level. However, our analysis of observations for the powerful VHE gamma-ray source Mrk 501 [13], detected at the  $11\sigma$  level, indicated that the accuracy of the estimated position of a VHE gamma-ray source decreases when DRO is used. Though using DRO enables us to efficiently select gamma showers against the background of showers from charged particles, the directions of the axes of the selected showers have relatively large errors. Therefore, we decided to repeat the analysis of the 1996 observations without using DRO.

The parameters of events registered simultaneously by each section were determined independently using the data for each section, so that each event had two values for each parameter, which we will label “1” for the northern section and “2” for the southern section. To reduce the background due to cosmic-ray particles, we applied a number of selection criteria based on the parameters of the Cerenkov events (Fig. 2).

In the selection, we considered first and foremost the total “energy” of the event  $V$  (the integrated light flux), which was measured over the same area as the second moments of the events in units of the analog-code converter quantization step. Events with amplitudes  $V(1) < 75$  units or  $V(2) < 125$  units were excluded from further consideration. Other parameters used to distinguish gamma-ray showers against the background of showers from charged particles (p showers) were the effective length and width of the image of the event. We excluded events from further consideration if at least one of the following conditions was fulfilled:  $A(1) > 0^\circ 33$ ,  $A(2) > 0^\circ 33$ ,  $B(1) > 0^\circ 23$ , or  $B(2) > 0^\circ 23$ .

As noted above, we also recorded the ultraviolet radiation of the events. The electrons from p showers with a given energy are known to penetrate, on average, to appreciably greater depths in the Earth’s atmosphere than those from gamma-ray showers with the same energy. Thus, Cerenkov events from p showers have considerably greater radiation fluxes at 200–300 nm (in the ultraviolet) [14]. We will call the ratio of an event amplitude at these wavelengths ( $U$ ) to the total amplitude in the visual ( $V$ ) the parameter UV. This parameter was first successfully used by us in our analysis of observations of the Crab Nebula [15].

On average, over all the years of observation, selection according to UV has improved the confidence of the detections up to the  $5.9\sigma$  level. Use of this parameter increases the signal-to-noise ratio by a factor of 2.5. The parameters  $A$ ,  $B$ ,  $V$ , and UV do not depend on the location of the event relative to the source, and are coordinate-independent.

Application of coordinate-dependent parameters (such as, for example, ALPHA; Fig. 1) enables us to increase  $Q$  (the signal-to-noise ratio) and improve our estimate of the direction toward the gamma-ray source. In this case, selection is performed for each section separately. Therefore, the set of events selected for one section only partially overlaps with the set for the other section. We can analyze such sets of gamma-like events in order to improve the coordinates of the gamma-ray source and more accurately determine the magnitude of the gamma-ray flux.

#### 4. RESULTS

To determine the direction of the incoming gamma-ray flux, we used a trial-source method [16–18]. This method is based on the fact that, in the focal plane of the telescope, the images of gamma-ray events are oriented toward the source, whereas the major axes of the image ellipses of p showers are oriented to first approximation uniformly in all directions. Let us suppose that we first select events adopting for the source direction an arbitrary point in the focal plane with coordinates  $X_i$  and  $Y_j$ , then make a selection using coordinate-dependent parameters. In this case, the number of remaining p showers will not depend on the adopted source position. At the same time, the number of images from gamma-ray showers will strongly depend on the adopted source position and will have a maximum in the direction toward the true source. In our case, the direction toward the source coincided with the center of the camera.

We can plot the distribution of the number of events selected over the field of view of the light detector as a function of the adopted source position  $N(X_i, Y_j)$ . This is essentially a “map”, or three-dimensional histogram, in which two dimensions are the Cartesian coordinates of the trial source relative to the center of the detector field of view, and the third dimension is the number of gamma-like events selected using a coordinate-depen-

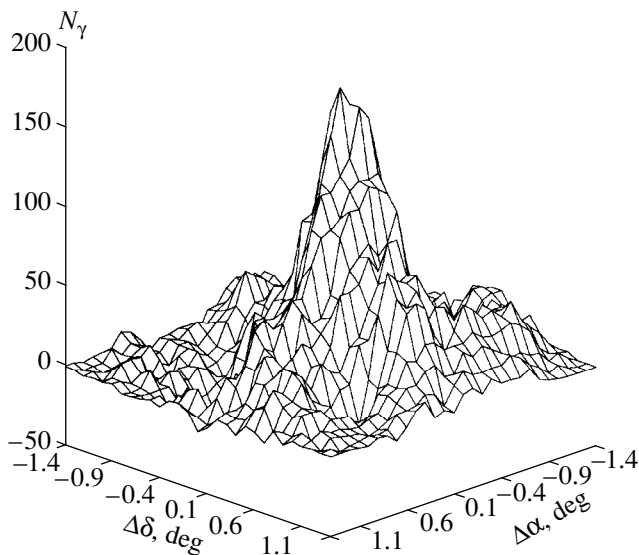


**Fig. 2.** Three-dimensional histogram for the selected gamma-ray events from 3C 66A.  $\Delta\delta$  is the deviation from the position of 3C 66A in declination, and  $\Delta\alpha$  is the deviation in right ascension (in deg).

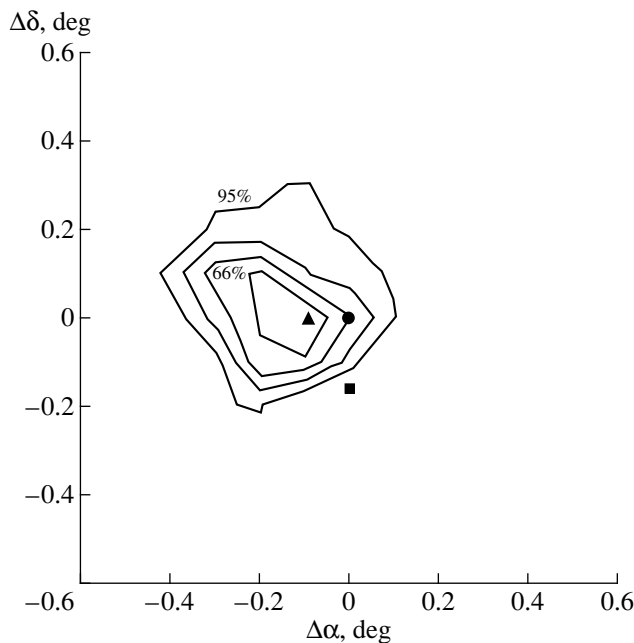


**Fig. 3.** Contours of  $N_\gamma$  for the gamma-ray source 3C 66A. Circle: position of the blazar 3C 66A; triangle: VHE gamma-ray source; square: gamma-ray source 3EG J0222 + 4253.  $\Delta\delta$  is the deviation from the position of 3C 66A in declination, and  $\Delta\alpha$  is the deviation in right ascension (in deg).

dent parameter. In this way, we can find the true position of the gamma-ray source. We have plotted such histograms for the data from both the northern and southern sections. We carried out the selection using both the coordinate-independent parameters noted above and the parameters DIST and MISS. DIST is

numerically equal to the angular distance from the event center of “gravity” to the trial source, and  $\text{MISS} = \text{DIST} \sin(\text{ALPHA})$  (Fig. 1). We set the limits on the values of these parameters  $\text{DIST}(1) < 0^\circ.9$  and  $0^\circ.25 < \text{DIST}(2) < 0^\circ.95$ . We excluded events with  $\text{MISS}(1) > 0^\circ.210$  and  $\text{MISS}(2) > 0^\circ.225$  for sections 1 and 2, respectively.

We can construct a total map from the maps for the two sections. Correct determination of the statistical error requires that events coincident at both sections be counted as a single event. Therefore, we found for each section gamma-like events  $N_c(X_i, Y_j)$  present in both sections, and also gamma-like events that, after selection in coordinate-dependent parameters, remained in the data for only the northern ( $N_1(X_i, Y_j)$ ) or southern ( $N_2(X_i, Y_j)$ ) section. In this case, the number of registered events identified as gamma rays in the on-source observations will be  $N_s(X_i, Y_j) = N_{c_s}(X_i, Y_j) + N_{1_s}(X_i, Y_j) + N_{2_s}(X_i, Y_j)$ . Similarly, this quantity for the background data will be  $N_b(X_i, Y_j) = N_{c_b}(X_i, Y_j) + N_{1_b}(X_i, Y_j) + N_{2_b}(X_i, Y_j)$ . We must map the background in order to exclude instrumental and methodical effects (see, for example, [17, 19]). The difference  $N_s(X_i, Y_j) - N_b(X_i, Y_j) = N_\gamma(X_i, Y_j)$  enables us to determine the coordinates of the gamma-ray source to within a few tenths of a degree. The position of the maximum of  $N_\gamma$  on the map corresponds to the direction toward the observed gamma-ray source. We can write the statistical error of  $N_\gamma$

$$\sigma = \sqrt{(N_{c_s} + N_{1_s} + N_{2_s}) + (N_{c_b} + N_{1_b} + N_{2_b})}.$$

Figure 2 presents the resulting three-dimensional histogram for the MISS criterion. The maximum value of  $N_\gamma = 172 \pm 29$  (corresponding to a  $5.9\sigma$  detection) has coordinates  $X_i = -0^\circ.1$  and  $Y_j = 0^\circ.0$ . During the observations, the center of the camera was pointed toward the blazar 3C 66A. Figure 3 shows the isophotes of  $N_\gamma$  for this histogram. The initial value of the isophote is drawn at the 95% significance level; this corresponds to an error box of  $0^\circ.50$ . The most probable location of the high-energy gamma-ray source 3EG J0222 + 4253 detected by EGRET [7] (the error box at the 95% significance level is  $0^\circ.31$ ) and the position of 3C 66A are plotted.

Visual observations [20, 21] show that, in October–November 1997, the brightness of 3C 66A decreased by approximately one magnitude compared to the same period in 1996, and a minor brightness increase was again observed in 1998. Analysis of our VHE observations (after selection of gamma-like events) shows that the gamma count rate was  $N_{96} = (0.290 \pm 0.053) \text{ min}^{-1}$  in 1996,  $N_{97} = (0.060 \pm 0.023) \text{ min}^{-1}$  in 1997, and  $N_{98} = (0.094 \pm 0.039) \text{ min}^{-1}$  in 1998. This implies that the gamma-ray flux from the direction toward 3C 66A appreciably decreased in 1997 and 1998 compared to 1996. A comparison of modeling results with the observa-

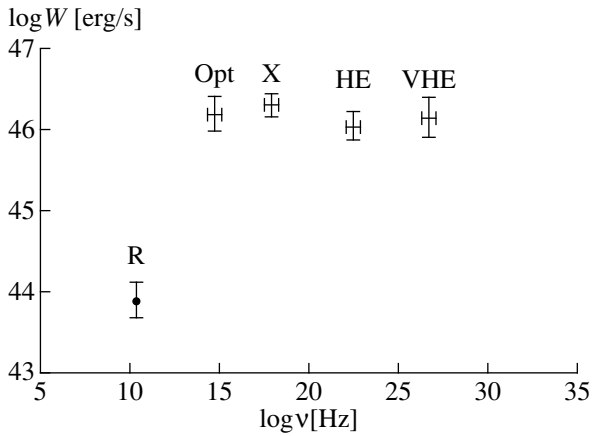


**Fig. 4.** Spectrum of the galaxy 3C 66A. The vertical segments indicate the intervals for flux variations. The horizontal axis plots the logarithm of the frequency, and the vertical axis plots the logarithm of the power per logarithmic frequency interval ( $\nu F$ ). R denotes radio emission, Opt optical emission, X X-ray emission, HE gamma rays with energies above 100 MeV, and VHE gamma rays with energies above 1 TeV.

tional data shows that, on average for the three years of observations, the flux of gamma rays with energies  $>1$  TeV was  $(3.0 \pm 0.9) \times 10^{-11}$  photons  $\text{cm}^{-2} \text{s}^{-1}$ .

## 5. CONCLUSIONS

Our multivariate analysis (using multiple parameters describing the Cerenkov events, both coordinate-independent and coordinate-dependent) enables us to state with a high degree of confidence (at about the  $6\sigma$  level) that there exists a VHE gamma-ray source ( $E_{\text{thr}} > 1.0$  TeV) toward the galaxy 3C 66A. The good coincidence of the gamma-ray source position derived using a trial-source method with that of the blazar 3C 66A further increases the trustworthiness of the results obtained. In 1997, we observed a decrease of the VHE gamma-ray flux from the object compared to its 1996 flux, simultaneous with a decrease in the visual brightness of 3C 66A; this may provide additional evidence that we have detected gamma-ray emission precisely from this source.

We note especially that, whereas the position of the high-energy gamma-ray source 2J 0220+4228 in the second EGRET catalog [6] differed from that of the VHE gamma-ray source detected by the GT-48 gamma-ray telescope by  $1^\circ$ , additional higher accuracy EGRET observations [7] yielded a position for the high-energy source 3J 0222 + 4253 that agrees within  $0^\circ.15$  with the position of the VHE gamma-ray source (Fig. 3) and the blazar 3C 66A. According to the EGRET data averaged over five years of observations, the flux of gamma rays with energies above 100 MeV is  $(18.7 \pm 2.9) \times 10^{-8}$  photons  $\text{cm}^{-2} \text{s}^{-1}$ . The differential spectral index is  $2.01 \pm 0.14$ . According to our data, the flux of gamma rays

with energies above 1 TeV is  $(3.0 \pm 0.9) \times 10^{-11}$  photons  $\text{cm}^{-2} \text{s}^{-1}$ . If we suppose that the spectral index does not change in this energy range, it is equal to  $-1.95$ , in good agreement with the data at 100 MeV. Of course, this comparison is not completely correct, since the gamma-ray flux from 3C 66A is variable at both 1 TeV and 100 MeV. Nevertheless, this result is of some interest.

According to Lanzetti [22], the redshift of 3C 66A is  $z = 0.444$ . If we assume that the gamma rays are emitted isotropically, their power is approximately  $10^{46}$  erg/s. On the one hand, this power may be strongly overestimated, since the VHE gamma-ray radiation is probably not isotropic, but it is rather difficult to estimate the degree of anisotropy of the radiation. On the other hand, at such great distances, the flux of gamma rays with energies  $>1$  TeV is strongly attenuated due to interactions with optical radiation in intergalactic space. According to the estimates of Stecker and de Jager [23], the flux of photons from 3C 66A with energies  $>1$  TeV is attenuated by a factor of about 200. Therefore, at present, it is not possible to provide a firm estimate of the source's true VHE power.

It is interesting to compare the power of the VHE emission of 3C 66A with its power at other frequencies. Figure 4 presents the power per logarithmic frequency band  $\nu F$  in the radio, optical, and X-ray, as well as the high-energy and VHE gamma-ray ranges [1, 7, 20]. It is striking that the power in all ranges except for the radio is approximately  $10^{46}$  erg/s. Note that the spectrum of 3C 66A is rather similar to that of the well-studied galaxy Mrk 501 (see, e.g., [24]), but its absolute power is two orders of magnitude higher. The similarity of the spectra suggests a common nature for these two objects and their radiation mechanisms.

## ACKNOWLEDGMENTS

The authors are grateful to the employees of the Crimean Astrophysical Observatory Z.N. Skiruta and S.G. Kochetkova for processing the observational data.

## REFERENCES

1. D. Maccagni, B. Garilli, R. Schild, and M. Tarenghi, *Astron. Astrophys.* **178**, 21 (1987).
2. M. Punch, C. W. Akerlof, M. F. Cawley, *et al.*, *Nature* **358** (6386), 477 (1992).
3. M. Catanese, C. W. Akerlof, S. Biller, *et al.*, in *Padova Workshop on TeV Gamma-Ray Astrophysics*, Ed. by M. Cresti, p. 348.
4. B. J. Wills and D. Wills, *Astrophys. J.* **190**, L97 (1974).
5. Yu. S. Efimov and N. M. Shakovskoy, in *Proceedings of the OJ-94 Annual Meeting, Perugia, Italie, Sept. 8–9, 1997*, Ed. by G. Tosti and L. Takalo, p. 24.
6. D. J. Thompson, D. L. Bertsch, B. L. Dingus, *et al.*, *Astrophys. J., Suppl. Ser.* **101**, 259 (1995).
7. R. C. Hartman, D. L. Bertsch, S. D. Bloom, *et al.*, *Astrophys. J., Suppl. Ser.* **123**, 79 (1999).

8. Yu. I. Neshpor, A. A. Stepanyan, O. R. Kalekin, *et al.*, Pis'ma Astron. Zh. **24**, 167 (1998) [Astron. Lett. **24**, 134 (1998)].
9. M. F. Cawley, J. Clear, D. J. Fegan, *et al.*, in *Proceedings of the 18th International Cosmic Ray Conference, Bangalore, India, 1983*, Vol. 1, p. 118.
10. B. M. Vladimirovskii, Yu. L. Zyskin, A. A. Korniyenko, *et al.*, Izv. Krym. Astrofiz. Obs. **91**, 74 (1995).
11. N. N. Chalenko, O. R. Kalekin, Yu. I. Neshpor, and A. A. Stepanyan, J. Astrophys. Astron. **18**, 151 (1997).
12. A. P. Korniyenko, A. A. Stepanyan, and Yu. L. Zyskin, Astropart. Phys. **1**, 245 (1993).
13. O. R. Kalekin, N. N. Chalenko, Yu. L. Zyskin, *et al.*, Izv. Ross. Akad. Nauk, Ser. Fiz. **63**, 604 (1999).
14. A. A. Stepanyan, V. P. Fomin, and B. M. Vladimirovskii, Izv. Krym. Astrofiz. Obs. **66**, 234 (1983).
15. O. R. Kalekin, Yu. I. Neshpor, A. A. Stepanyan, *et al.*, Pis'ma Astron. Zh. **21**, 184 (1995) [Astron. Lett. **21**, 163 (1995)].
16. C. W. Akerlof, M. F. Cawley, M. Chantell, *et al.*, Astrophys. J. Lett. **377**, L97 (1991).
17. Yu. I. Neshpor, A. P. Korniyenko, A. A. Stepanyan, and Yu. L. Zyskin, Exp. Astron. **5**, 405 (1994).
18. V. P. Fomin, S. Fennell, R. C. Lamb, *et al.*, Astropart. Phys. **2**, 151 (1994).
19. A. P. Korniyenko, Yu. I. Neshpor, Yu. L. Zyskin, and A. A. Stepanyan, Izv. Krym. Astrofiz. Obs. **93**, 143 (1996).
20. L. O. Takalo, T. Parsimo, A. Sillanpaa, *et al.*, [http://bldata.pg.infn.it/volume\\_1/6/6.html](http://bldata.pg.infn.it/volume_1/6/6.html) (1999).
21. Yu. S. Efimov, personal communication (1999).
22. K. M. Lanzetta, D. A. Turnshek, and J. Sandoval, Astrophys. J., Suppl. Ser. **84**, 109 (1993).
23. F. W. Stecker and O. C. de Jager, in *Proceedings of the Kruger National Park Workshop on TeV Gamma-Ray Astrophysics*, Ed. by O. C. de Jager, p. 39.
24. J. Kataoka, J. R. Mattox, J. Quinn, *et al.*, Astropart. Phys. **11** (1–2), 149 (1999).

*Translated by G. Rudnitskii*